

## RESEARCH ARTICLE | *Control of Movement*

# Task-dependent vestibular feedback responses in reaching

 Johannes Keyser,  W. Pieter Medendorp, and  Luc P. J. Selen

*Radboud University Nijmegen, Donders Institute for Brain, Cognition and Behaviour, Nijmegen, The Netherlands*

Submitted 16 February 2017; accepted in final form 28 March 2017

**Keyser J, Medendorp WP, Selen LP.** Task-dependent vestibular feedback responses in reaching. *J Neurophysiol* 118: 84–92, 2017. First published March 29, 2017; doi:10.1152/jn.00112.2017.—When reaching for an earth-fixed object during self-rotation, the motor system should appropriately integrate vestibular signals and sensory predictions to compensate for the intervening motion and its induced inertial forces. While it is well established that this integration occurs rapidly, it is unknown whether vestibular feedback is specifically processed dependent on the behavioral goal. Here, we studied whether vestibular signals evoke fixed responses with the aim to preserve the hand trajectory in space or are processed more flexibly, correcting trajectories only in task-relevant spatial dimensions. We used galvanic vestibular stimulation to perturb reaching movements toward a narrow or a wide target. Results show that the same vestibular stimulation led to smaller trajectory corrections to the wide than the narrow target. We interpret this reduced compensation as a task-dependent modulation of vestibular feedback responses, tuned to minimally intervene with the task-irrelevant dimension of the reach. These task-dependent vestibular feedback corrections are in accordance with a central prediction of optimal feedback control theory and mirror the sophistication seen in feedback responses to mechanical and visual perturbations of the upper limb.

**NEW & NOTEWORTHY** Correcting limb movements for external perturbations is a hallmark of flexible sensorimotor behavior. While visual and mechanical perturbations are corrected in a task-dependent manner, it is unclear whether a vestibular perturbation, naturally arising when the body moves, is selectively processed in reach control. We show, using galvanic vestibular stimulation, that reach corrections to vestibular perturbations are task dependent, consistent with a prediction of optimal feedback control theory.

vestibulomotor; feedback control; galvanic vestibular stimulation; minimum intervention principle

IN MOST DAILY CIRCUMSTANCES, we can effortlessly navigate through the environment and simultaneously reach for an object, such as reaching for a cocktail while passing a waiter. While both actions and their coordination may be planned ahead, we have to rely on sensory feedback control in case somebody unexpectedly bumps into us while we're reaching for the glass. To investigate the properties of such online corrections experimentally, reaching movements are typically perturbed mechanically, by imposing an external force on the arm, or visually, by displacing the representation of the target or hand. Various studies have shown that even early feedback

corrections are remarkably sophisticated, taking into account the relevance of the perturbation for task performance (Franklin and Wolpert 2008), the urgency to react (Crevecoeur et al. 2013; Oostwoud Wijdenes et al. 2011), and the spatial layout of the target (Knill et al. 2011; Nashed et al. 2012; Pruszynski et al. 2008).

Optimal feedback control (OFC) provides a powerful theoretical framework for interpreting these sophisticated, task-dependent, feedback responses (Scott 2004; Todorov and Jordan 2002). Within this framework, online corrections are manifestations of an optimal control policy that generates motor output based on a state estimate which in turn is informed by sensory input. The control policy reflects the optimal tradeoff between the constraints of the neuromusculoskeletal system, like its noise levels and dynamics, movement effort, and task requirements such as target size. As a result, an OFC controller will largely allow task-irrelevant perturbations without correction, also referred to as the minimum intervention principle. In direct support, reaching movements to targets of different shapes are corrected less for visual or mechanical perturbations along the task-irrelevant than the task-relevant spatial dimension (Knill et al. 2011; Nashed et al. 2012; Pruszynski et al. 2008).

Does the minimum intervention principle also apply to the integration of vestibular feedback signals into the control policy for goal-directed reaching movements? Bresciani et al. (2002c) have shown that subjects successfully integrate vestibular and proprioceptive signals to correct an ongoing arm movement during passive whole-body rotation without visual cues, compensating for effects of arm inertia and induced Coriolis forces. In addition, Bockisch and Haslwanter (2007) reported similar reach corrections in response to a vestibular aftereffect induced by abruptly stopping an ongoing rotation, thus eliminating proprioceptive cues. Likewise, Guillaud et al. (2011) reported appropriate reach corrections for passive whole-body rotation in a proprioceptively deafferented patient, suggesting that vestibular feedback is sufficient to make appropriate responses. Despite these insights, it remains unclear whether these vestibularly mediated corrections are dedicated to stabilize the hand in space irrespective of the reach goal, or whether they are tuned to the specific constraints imposed by the reaching task.

In this study, we investigate the sophistication of vestibular mediated reach responses by using bilateral, bipolar galvanic vestibular stimulation (GVS), which delivers a small current through electrodes placed on the left and right mastoid processes. Although an artificial stimulus, GVS induces an illu-

Address for reprint requests and other correspondence: J. Keyser, Donders Institute for Brain, Cognition and Behaviour, Radboud University Nijmegen, P.O. Box 9104, NL-6500 HE, Nijmegen, The Netherlands (e-mail: j.keyser@donders.ru.nl).

sory whole-body rotation by directly exciting the vestibular afferents (Fitzpatrick and Day 2004), without activating other sensory modalities or inducing passive forces on the arm like an actual rotation of the body (Bresciani et al. 2002c; Guillaud et al. 2011).

Several studies have already shown that GVS alters reach trajectories to memorized, earth-fixed targets, as if the feedback controller compensates for the illusory motion of the body (Bresciani et al. 2002a, 2002b; Mars et al. 2003; Moreau-Debord et al. 2014). However, the level of sophistication of the vestibular integration into the arm's ongoing reach control remains unclear. In our experiment, we tested whether vestibular feedback is processed task dependently, based on the behavioral goal. Healthy participants received GVS while they reached either to a narrow or a wide target of which the left-right dimension was irrelevant. Based on the OFC framework, we predicted a reduction of GVS-evoked feedback responses when reaching to the wide target compared with the narrow target. This would suggest that the corrections are governed by a task-dependent feedback controller that evaluates vestibular inputs in relation to the reach constraints.

## METHODS

**Participants.** Twenty-four subjects (14 women; age 21–34 yr) participated in the experiment. All subjects but one (this person performed the task with his nonpreferred hand) were right-handed, and all gave written, informed consent. All subjects had normal or corrected-to-normal vision and reported to have no known vestibular or motor deficits. The study was part of a research program approved by the ethics committee of the Social Sciences faculty of the Radboud University in Nijmegen, The Netherlands. Subjects were reimbursed for their time by payment (10 €/h) or by course credit. One of the 24 subjects was excluded from analyses due to failure to comply with the timing requirements of the task (see *Data analysis*).

**Experimental setup.** Subjects sat in front of a planar robotic manipulandum (vBOT; Howard et al. 2009), as shown in Fig. 1, *A* and *B*. The right arm rested on an air sled floating on a glass top table, while the left arm rested on the left thigh. Subjects performed reaches with the right hand, while holding the handle of the manipulandum. The manipulandum in combination with the air sled restricted the reaches to the horizontal plane. Subjects wore computer-controlled, liquid crystal shutter glasses (Translucent Tech) to totally block vision in GVS trials. Visual stimuli were presented in the plane of movement via a semisilvered mirror, reflecting the display of an LCD monitor (model VG278H, Asus) suspended above. The mirror prevented subjects to see their arm. All visual stimuli, i.e., the start location of the reach, the target, and feedback about task performance were projected into the plane of movement. Hand position, derived from the handle position, was presented as a circular cursor. Hand position was monitored and stored at 1,000 Hz, whereas the hand cursor position was displayed at 120 Hz on the LCD monitor.

Subjects had to lean forward with their body, pitching their heads down, using a soft head rest, shoulder straps, and a foot rest for support. In this pitched position, GVS is mainly interpreted as a body vertical-axis (yaw) rotation, which causes larger reach trajectory deviations than with the head upright (Moreau-Debord et al. 2014). Pitch angles, estimated from photographs, ranged from 41 to 56° with respect to the direction of gravity.

Bilateral, bipolar GVS was applied by electrodes attached to the mastoid processes. The current was delivered by a linear, insulated stimulator (model STMISOLA, Biopac) through disposable, self-adhesive electrodes with a gel cavity of 16 mm diameter (Biopac model EL509). The electrode sponges were filled with salt-free, electrically conductive gel. Before attachment, the skin was cleansed with 70% alcohol solution.

The electronic stimulator acted as a current source, with its output waveform being a scaled version of the hand speed during the reach. The output current was updated at a rate of 1,000 Hz. The GVS-gain of this speed-to-current conversion was 0.055 mA·s/cm. This gain was chosen empirically such that the result would typically peak at 2.5 mA, based on a bell-shaped speed profile that peaks at 45 cm/s (see

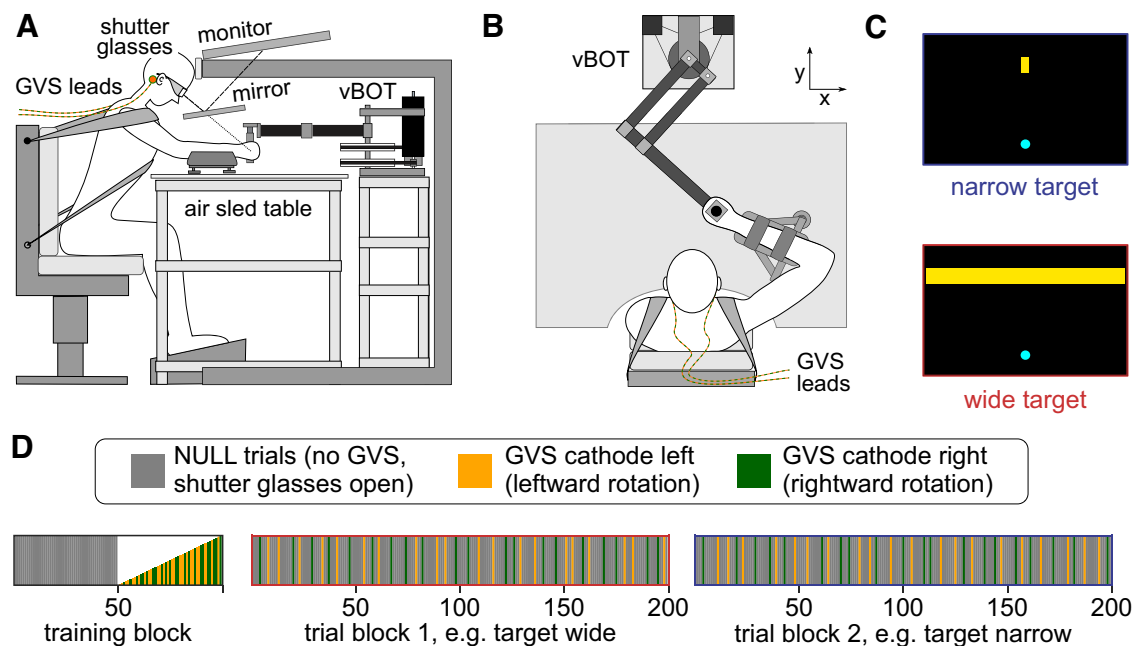


Fig. 1. Experimental setup. *A* and *B*: subject sits with the head inclined forward, holding the handle of a robotic manipulandum (vBOT). Visual stimuli are presented through a mirror. GVS electrodes were attached to both mastoids. *B*: top view of the setup, with the virtual image of the wide target. *C*: images of the two different reach targets, narrow and wide; not to scale. *D*: trial order. After training, there were two blocks of 200 trials per target condition, counterbalanced across subjects, during which NULL and GVS trials were interleaved pseudo-randomly.

RESULTS). To avoid excessive peak currents, the output was clipped to 3 mA, which happened in only 2.8% of all GVS trials.

**Experimental paradigm.** Subjects performed 20-cm reaching movements in the midsagittal plane from a central start position to either a narrow or a wide target. The target was a yellow rectangle, with a depth of 2 cm and a width of either 1 or 60 cm, referred to as the narrow and wide targets, respectively (Fig. 1C). The instructions were to finish the reach anywhere on the target, using a single smooth movement within the requested time interval ( $700 \pm 75$  ms). For the wide target this effectively means that there was no lateral constraint on the reach end point.

Before a trial started, subjects were asked to place the hand cursor (white circle of 0.6 cm diameter) within the start position (a cyan circle of 1.2 cm diameter). After 1 s, a beep prompted subjects to reach toward the target. As soon as the reach was detected (handle speed  $> 5$  cm/s), the cursor disappeared. In case the reach was not initiated within 1 s, a red screen appeared with the text “Move after beep” and the trial would be repeated. For the purpose of task feedback during the experiment, reach durations within an interval of  $700 \pm 75$  ms were considered correct. If a reach took longer, a low-pitched beep was played back and a text “Too Slow” appeared on screen. Analogously, if a reach was too fast, the beep was high-pitched and the text was “Too Fast.” These messages were used to encourage consistent reaching throughout the experiment but did not lead to an actual rejection of the trial. After the messages were shown, subjects were asked to relax their arm so the manipulandum could transport their hand back to the start location. Robot forces were calculated based on a PD controller in which set point followed a minimum-jerk trajectory toward the start location with a duration of 650 ms.

Subjects performed reaches in which GVS was absent (NULL trials) and in which GVS was administered (GVS trials). The end position of a reach was defined as the first point where the handle speed was  $< 5$  cm/s. In NULL trials, feedback about reach accuracy was given by displaying the end position of the reach for 1 s. In the narrow target condition, the reach end point was displayed as a circle of 0.6-cm diameter. In the wide target condition, performance feedback was only provided in the fore-aft direction by displaying a thin line with a thickness of 0.6 cm that spanned the entire width of the target (60 cm). This prevented subjects from gaining feedback about their lateral end position and forced them to only care about the reach accuracy in the fore-aft dimension. If the reach ended within the target area, the target color changed from yellow to green, and if the target was missed, its color changed to red. For reaches with correct timing, an additional text was displayed. If the target was hit, the text stated “Great”; otherwise it stated “Move to Target.” In case the reach timing was not according to instructions, subjects only received feedback about their timing (by a beep and text; see above).

In GVS trials, a bipolar GVS current was administered during the reach, with its amplitude proportional to the handle speed. We chose these state-dependent GVS currents to generate smooth stimulation profiles for the vestibular system, like in natural coordinated movements of trunk and arm (Pigeon et al. 2003). As soon as the reach onset was detected (handle speed  $> 5$  cm/s), the shutter glasses closed to prevent visual feedback of the cursor or allocentric cues. The shutter glasses opened again when the handle speed fell  $< 5$  cm/s. No feedback about reach accuracy was given in GVS trials, i.e., the target color always remained yellow. In case of incorrect timing, the same feedback was given as in NULL trials. In a single trial, the current never switched polarity as it was based on speed (always positive) and a positive or negative GVS-gain.

The main experiment comprised two blocks of 200 trials (Fig. 1D). In one, subjects reached to the narrow target; in the other block they reached to the wide target. The order of these conditions was counterbalanced across subjects. Both blocks had 160 NULL trials and 40 GVS trials. The GVS trials were pseudo-randomly interleaved, such that each GVS trial was followed by two to six (on average four)

NULL trials. On half of the GVS trials the cathode was on the subject's left mastoid, simulating leftward rotation. In the other half, the cathode was on the right, simulating rightward rotation. The polarity was chosen pseudo-randomly, such that a given polarity occurred maximally in two consecutive GVS trials. After every 50 trials, a break of minimally 1 min was introduced. Between the two blocks of different target width, there was a break of  $\sim 5$  min.

Prior to the experiment, subjects completed two to four sets of 25 trials to get acquainted with the reach task, practicing the target condition that was tested first in the actual experiment. During this training period, 80% of trials were NULL trials (see above) and in the other 20% of trials the shutter glasses closed at reach onset. Once subjects were able to reach to the target within the expected time interval, we familiarized them with the GVS trials, using an additional set of 50 trials. In each trial, subjects reached to the remembered target location (shutter glasses closed at the start of the reach), while the handle speed determined the stimulation waveform. The GVS-gain of the speed-to-current conversion increased by 2% every trial (i.e., by 0.0011 mA·s/cm per trial), running from 0 to 100% over these 50 trials, and its polarity was randomly chosen. The final GVS-gain of 0.055 mA·s/cm (i.e., 100%) was used in all subsequent GVS trials in the main experiment. Subjects' well-being was monitored especially during these familiarization trials and any indication of adverse effects would have resulted in cancellation of the experimental session. There were no cancellations of the experiment for any reason.

**Data analysis.** Analyses were performed with Python 3.4 (Python Software Foundation, <https://python.org>), including packages h5py (HDF Group 1997–2017), numpy (van der Walt et al. 2011), matplotlib (Hunter 2007), and scipy (Jones et al. 2001–2017). Statistical tests were done using R 3.3 (R Core Team 2016) via the rpy package (<http://rpy2.bitbucket.org/>).

Reach onsets and offsets were determined using a velocity threshold of 5 cm/s. Reaches with a duration outside a  $700 \pm 150$ -ms time interval were excluded, even though during the experiment subjects received timing feedback based on a tighter time window of  $700 \pm 75$  ms. One subject was excluded from the analyses because even the relaxed timing criterion of 150 ms led to the exclusion of 178 trials (45%). For the remaining group ( $N = 23$ ), this criterion led to an average exclusion of 7.2 trials.

Position and velocity traces were linearly interpolated between reach onset and offset and were subsampled to contain 100 samples, i.e., reach duration was normalized to a 0–100% range. Hand position at reach onset of each trial was subtracted to align all starting points. To quantify the extent to which GVS perturbed the reach trajectories, we calculated the perpendicular distance between hand positions and a straight line connecting the start location and the average end point of all NULL trials, per subject and target condition. In other words, all trajectories of a given subject and target condition were rotated by the same amount, such that straight-ahead corresponded to the average reach end point of NULL trials. This allowed us to quantify GVS-evoked corrections in terms of the perpendicular distance from the average nonperturbed reach direction.

We examined whether GVS affects reach trajectories differently in the two target conditions (narrow vs. wide). First, we analyzed GVS trials in isolation from the NULL trials. However, this direct comparison of GVS trials from the two target conditions might be unwarranted because the target conditions already differ in their NULL trials. The wide target condition shows a more dispersed trajectory distribution compared with the narrow target condition (see Nashed et al. 2012, and RESULTS). Therefore, we also examined the effect of GVS on reach behavior by subtracting from each trial the average of 10 NULL trials whose initial trajectories (the first 20% of the reach) were most similar to this GVS trial (see Fig. 2B). The resulting deviations yield an estimate of the GVS-evoked trajectory corrections while accounting for the differences between target conditions that are already apparent in the NULL trials. The similarity between two trajectories was defined as the reciprocal of the root mean squared



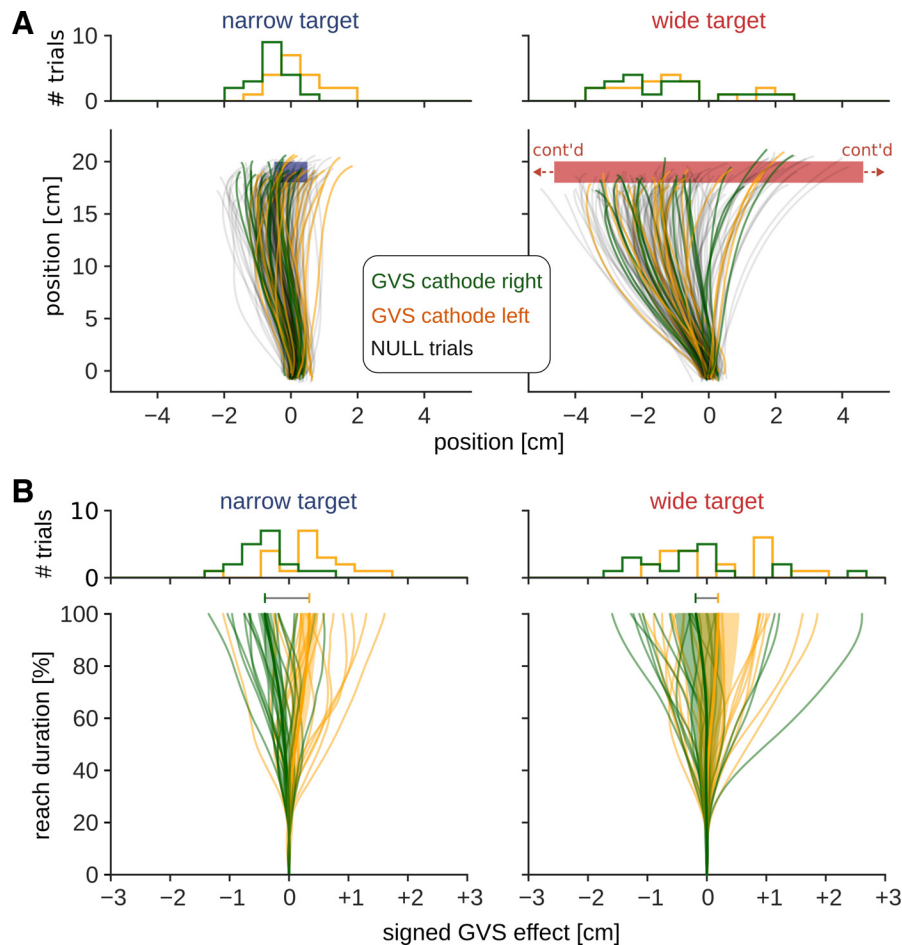


Fig. 2. Raw data and preprocessed data from one example subject. **A:** raw position traces to the narrow target (*left*) and wide target (*right*). Histograms show distribution of horizontal positions of the reach end points for the two GVS polarities. *cont'd*, Continued. **B:** GVS-evoked perpendicular deviations relative to the average of the 10 most similar NULL trials, from the same subject. Vertical axis denotes normalized reach duration (with a mean of  $\sim 700$  ms). Thin lines show the individual trajectories of GVS trials. Bold lines and shadings indicate the mean  $\pm 1$  SE in lateral direction. Histograms show distribution of NULL-corrected reach end points.

(RMS) error between their perpendicular deviations, i.e., a higher RMS error corresponds to a lower similarity. We restricted the similarity computation until 20% of normalized time [until 145 ms (7 SD)], to avoid the inclusion of the earliest effects of GVS, which are detectable at  $\sim 176$  ms after a step input (Moreau-Debord et al. 2014).

The setting of  $n = 10$  most similar NULL trials was chosen because it provided the lowest error for predicting NULL trials in a cross-validation procedure. To arrive at this number, for every NULL trial's position trace and the average of its  $n$  most similar NULL trials, the RMS error between them was computed along all time points, i.e., beyond the time point ( $t = 20\%$ ) used for the similarity computation. We computed the mean of RMS errors across subjects on a grid containing  $n = 1-4, 5, 10, 15, \dots, 160$  (the maximum) trials and found  $n = 10$  to result in the minimum prediction error. We also performed a velocity-based matching procedure, again with  $n = 10$  for computing the most similar NULL trajectory. Note that, for most parameter settings of the matching procedure ( $t \geq 5\%$  and  $n > 5$ ), the conclusion from this analysis agrees with the findings from the direct analysis that does not involve any matching with NULL trials. Since this matching procedure accounts for different dispersions in NULL trials between target conditions (see RESULTS), all further results on GVS trials pertain to them.

To ensure the existence of matching NULL traces surrounding each GVS trace, we rejected GVS trials if their perpendicular deviation from the average NULL trajectory exceeded  $\pm 3$  standard deviations from the distribution of NULL trials in the same condition, along the first 30% of the trial. Across subjects, this led to an average of 0.7 rejected GVS trials.

To quantify the time-dependent, combined effect of GVS with cathode left and cathode right, we computed, per subject and target condition, the difference between the average response of GVS trials

with the cathode on the left and with the cathode on the right. This also removes any systematic influences due to closing the shutter glasses.

To quantify onset times of the corrective responses to GVS, we used an extrapolation method, introduced by Veerman et al. (2008) and evaluated to yield accurate estimates in simulations by Oostwoud Wijdenes et al. (2014). For our purpose, we interpolated the velocity trace of the total GVS effect between the points of 25 and 75% of its peak value. The onset of the GVS effect was defined as the time point when the extrapolation of this line crosses zero. For two subjects, this method resulted in a negative onset of the GVS effect, i.e., before the start of the reach, and we excluded these from the onset time analysis.

We summarized all data by their mean and standard deviation (SD). For normally distributed data, statistical tests were done using (paired)  $t$ -tests. We assessed the  $t$ -test's assumption of normality with Shapiro-Wilk test. Statistical tests were evaluated against a two-tailed alternative hypothesis, unless noted otherwise. RESULTS were considered significant at an alpha level of 0.05.

To evaluate the effects of GVS and target condition on the hand's perpendicular position and velocity traces, we performed running, one-tailed  $t$ -tests. Running tests were considered significantly different if they were continuously significant for longer than 100 ms (i.e.,  $>18\%$  of normalized reach duration). To further avoid the multiple comparisons problem, we complemented the running  $t$ -tests with single  $t$ -tests on the maximum deviation in terms of velocity and on the position deviation at the end of the reach.

## RESULTS

Our experiment was designed to test whether vestibular perturbations, evoked by GVS, during goal-directed reaching

result in task-dependent corrections of the reach trajectories and are not aimed at stabilizing the hand in space. Subjects reached either toward a narrow or a wide target (target conditions narrow vs. wide). In 20% of trials, a GVS current was administered to supposedly evoke an illusory body motion, especially rotation (Fitzpatrick and Day, 2004; Reynolds and Osler, 2012), resulting in an online correction of the reach (e.g., Moreau-Debord et al. 2014). We hypothesized that these corrections would be smaller for reaches to the wide than to the narrow target.

Figure 2A presents reach trajectories of an example subject in both target conditions. Black traces represent the NULL trials; green and orange traces indicate the GVS trials (cathode left vs. right, respectively). While NULL traces generally straddle along the forward direction for reaches to the narrow target, they show substantial dispersion when reaching to the wide target, perhaps due to a lack of feedback about the lateral position of the reach end point. This increased spread of reach end points was seen in all participants, consistent with previous observations (Nashed et al. 2012). We quantified this observation by calculating the standard deviations of the reach end points, which were significantly different between target conditions [narrow: 0.71 cm (0.12 SD), wide: 1.07 cm (0.35 SD);  $t(22) = -5.65$ ,  $P = 0.00001$ ].

When analyzing the effects of target condition on GVS, we removed any possible influence of this difference in end point dispersion, by calculating the difference between each GVS trial and its 10 most similar NULL trials (see *Data analysis*). Figure 2B provides the perpendicular deviation of the individual GVS trials relative to their corresponding NULL trials as a function of normalized reach duration. Superimposed are the respective means. For this subject, the difference between the mean trajectories for GVS cathode left and right is larger for reaches to the narrow than to the wide target.

In line with the single-subject results in Fig. 2B, Fig. 3A shows that opposite GVS polarities also evoke distinct reach corrections when averaged across subjects, plotted as a function of normalized reach duration. Opposite polarities of GVS result in a wider separation for the narrow target compared with the wide target. Figure 3B summarizes these signed GVS effects per condition as the total GVS-evoked corrective responses (cathode left minus right). At the reach end points, these total GVS-evoked corrective responses had a magnitude of 0.57 cm (0.41 SD) for the narrow condition and 0.38 cm (0.36 SD) for the wide target (33% reduction). For both target conditions these corrections were significantly different from zero [one-sample, one-tailed  $t$ -tests; narrow:  $t(22) = 6.47$ ,  $P = 0.000001$  and wide:  $t(22) = 5.00$ ,  $P = 0.00003$ ]. More importantly, the GVS effect on the reach end points was significantly greater in the narrow compared with the wide condition [paired, one-tailed  $t$ -test,  $t(22) = 2.46$ ,  $P = 0.01$ ]. This effect is shown in Fig. 3C, which depicts the average paired difference between the total GVS effects in the wide and narrow condition and the SE across subjects. Running one-tailed  $t$ -tests reveal that the total GVS effects were significantly greater than zero for 74 and 85% of the normalized reach duration in the narrow and wide conditions, respectively. The magnitude in the narrow condition was significantly larger than in the wide condition for 29% of the movement duration (paired, one-tailed running  $t$ -tests). This supports

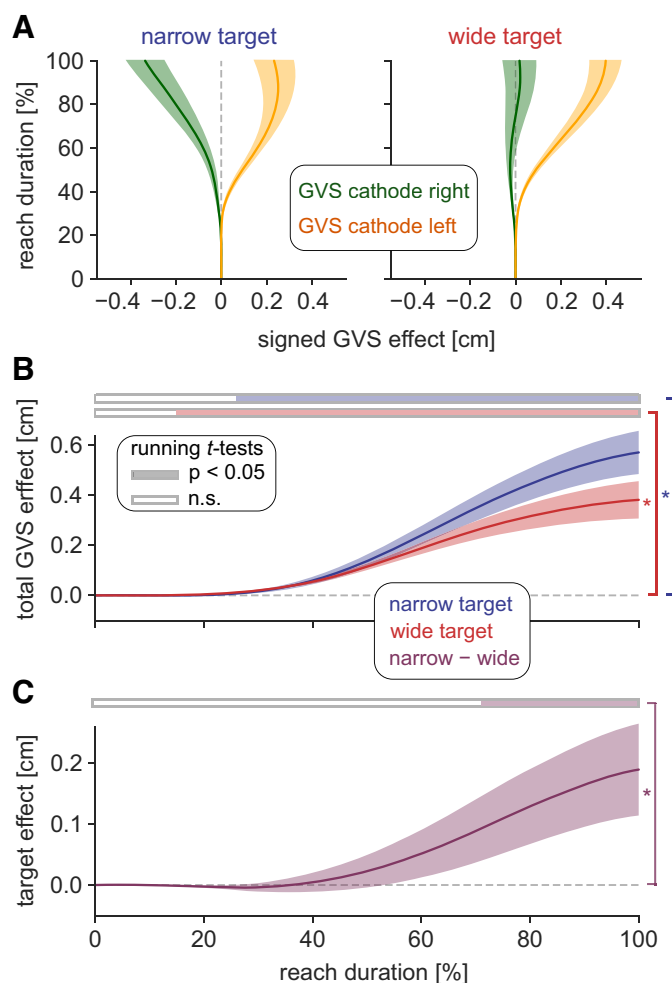


Fig. 3. Group-level comparison of GVS-evoked position corrections. Lines and shaded areas denote mean  $\pm$  1 SE across subjects. Bars denote significant running, paired, one-tailed  $t$ -tests; \*denotes significance for >100 ms. A: GVS-evoked position corrections per GVS polarity and target condition. B: total GVS effect (cathode left minus right) on position, per target condition. n.s., Not significant. C: target effect on total GVS effects (condition narrow minus wide), for perpendicular positions.

our main hypothesis that corrections are task dependent, and hence become smaller if task constraints in the perturbation direction are relaxed.

For a closer examination of the GVS effects over time, Fig. 4 plots the velocity of the corrective responses, i.e., of the NULL-corrected velocity traces of the GVS trials. This presentation shows a similar pattern as already seen in the position domain. In both target conditions, the total GVS effects were significantly greater than zero for 83 and 80% of the movement time in the narrow and wide conditions, respectively (Fig. 4B, running one-tailed  $t$ -tests,  $P < 0.05$ ). The effect was also stronger for the narrow than the wide target, as shown in Fig. 4C, indicating that the velocity traces differ significantly for 47% of the movement duration (paired, one-tailed running  $t$ -tests). To compare these differences in a single statistical test, we examined the task-dependent GVS effects at peak velocity of the corrective responses. Peak velocity of the corrective response in the narrow condition was 1.86 cm/s (1.15 SD) and 1.40 cm/s (0.81 SD) in the wide condition. This amounts to a significant [paired, one-tailed  $t$ -test,  $t(22) = 2.26$ ,  $P = 0.02$ ]

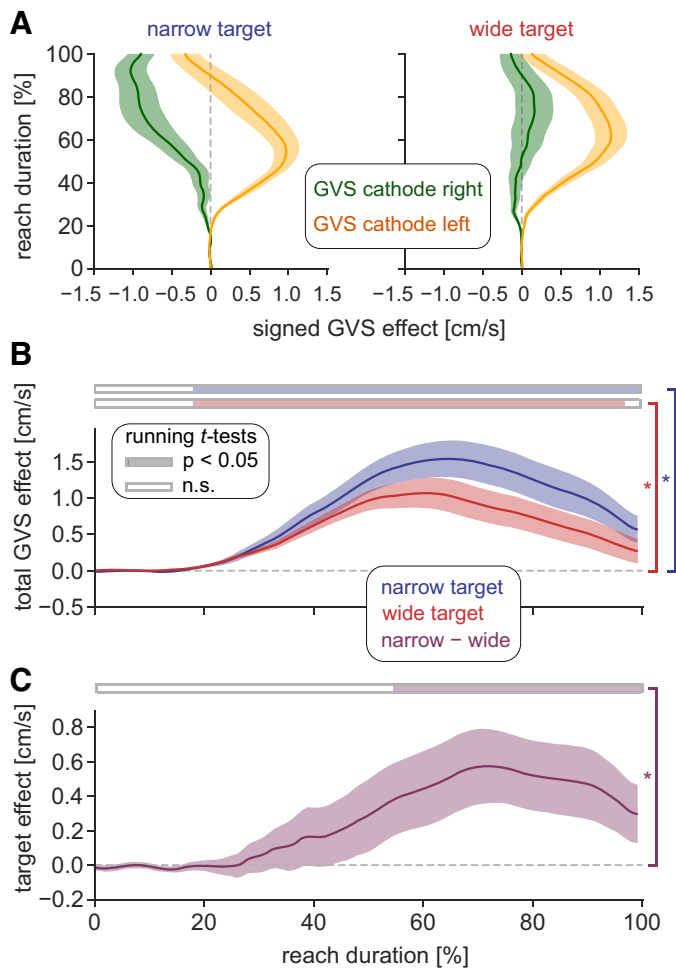


Fig. 4. Group-level comparison of GVS-evoked velocity corrections. Format as in Fig. 3.

reduction by 25% of the corrective response for the wide compared with the narrow condition.

Finally, we examined onset times of the GVS-evoked corrections. Two subjects were excluded from this analysis because the estimated onset times of the corrections appeared negative (see METHODS). The correction onsets in terms of average percentage of the total trial duration were 26.28% (11.09 SD) and 23.61% (6.65 SD) for narrow and wide target, respectively. These values were not significantly different [paired  $t(20) = 0.52$ ,  $P > 0.6$ ]. In terms of actual time, the pooled mean of 24.95% corresponds to an average onset time of 181 ms (9 SD), in line with findings by Moreau-Debord et al. (2014).

To conclude that the corrective responses to GVS were larger in the narrow than in the wide condition, it is important that the stimulation itself was not larger for the narrow compared with the wide condition. First, we tested for differences in the mean and peak values of absolute GVS currents. Neither was significantly greater in the narrow condition, i.e., the mean current was 1.56 mA (0.07 SD) in both conditions [paired, one-tailed  $t(22) = -0.09$ ,  $P > 0.5$ ], the peak current was 2.47 mA (0.14 SD) vs. 2.44 mA (0.12 SD) [paired, one-tailed  $t(22) = 1.35$ ,  $P > 0.09$ ]. As a corollary, this means that reach speeds during GVS trials were also not higher in the narrow target condition. Furthermore, reach durations did not differ

between target conditions [mean 719 ms (35 SD), paired  $t(22) = 1.37$ ,  $P > 0.1$ ]. Finally, we tested whether there were parts of the entire trace of GVS currents that differed between the two target conditions (Fig. 5). One-tailed, running  $t$ -tests indicate that there were no greater GVS currents in the narrow condition since they were significant only for 5% of normalized reach duration. In conclusion, the difference in the observed correction amplitudes for the two target conditions was not due to differences in the GVS currents but can be related to differences in the task constraints.

## DISCUSSION

Our main finding is that the GVS-evoked corrective responses are task dependent, i.e., corrective responses to the same vestibular stimulation are different for different target widths. Reach duration and peak velocity did not differ between the two target conditions, resulting in the same vestibular stimulation. The onset of the corrective responses did not differ between target conditions, but subjects showed ~33% smaller corrections, in terms of the end point, when reaching to the wide target compared with the narrow target. This modulation of feedback responses by target width suggests that vestibular inputs are part of a feedback control policy that is set up for the specific task demands, in agreement with predictions from OFC theory (Todorov and Jordan 2002).

In our study, we built on previous results showing that, relative to control trials, GVS evokes reach corrections away from the cathodal stimulation side (Bresciani et al. 2002b; Mars et al. 2003; Moreau-Debord et al. 2014). We made similar observations in the narrow condition (Fig. 3). At reach end points, we found average corrections away from the cathodal stimulation side of 0.34 cm (0.41 SD) and 0.23 cm

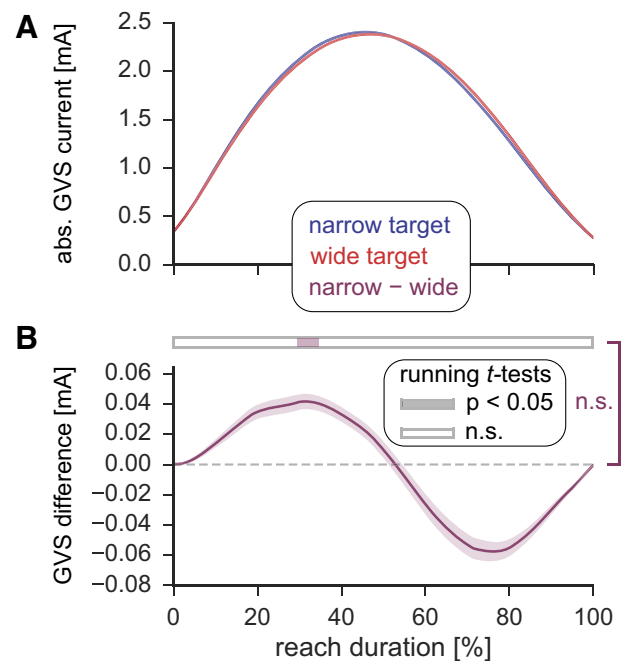


Fig. 5. Comparison of GVS current waveforms between target conditions. Lines and shaded areas denote mean  $\pm$  1 SE across subjects. A: absolute (abs.) GVS currents per target condition, almost overlapping along each point in time. B: difference between absolute GVS currents, condition narrow minus wide. Bars denote significant running, paired, one-tailed  $t$ -tests.



(0.42 SD) for cathode right and left, respectively. Bresciani et al. (2002b) report deviations of 0.40 and 0.76 cm for cathode right and left, respectively (based on their reported 0.66 and 1.24° with a larger target distance of 35 cm). Moreau-Debord et al. (2014) report corrections of  $0.39 \text{ cm} \pm 0.11 \text{ SE}$  for cathode right and  $0.68 \text{ cm} \pm 0.12 \text{ SE}$  for cathode left, for 20-cm reaches. Note that all previous studies used constant stimulation (Bresciani et al. 2002a, 2002b; Mars et al. 2003; Moreau-Debord et al. 2014). Instead, we used GVS currents in proportion to the hand speed, resulting in smooth, bell-shaped stimulation profiles that mimic natural movements in which trunk and arm start and stop moving at similar time points (Pigeon et al. 2003), but note that at the canal afferents GVS does not correspond to a natural head rotation (Fitzpatrick and Day 2004). Nevertheless, the onset of the GVS-evoked velocity corrections (181 ms) was nearly identical to the 176 ms reported in the study by Moreau-Debord et al. (2014). This close correspondence is perhaps surprising since our stimulation magnitude at reach onset (handle speed  $>5 \text{ cm/s}$ ) was only  $\sim 0.3 \text{ mA}$  and peaked at  $\sim 2.5 \text{ mA}$ , while Moreau-Debord et al. (2014) used a square pulse of 3 mA.

Our finding that the online feedback responses were modulated by the behavioral goal provides evidence that vestibular inputs feed directly into the reach controller. The task dependency of the responses challenges the contention that vestibular-evoked corrections are intended to stabilize the hand in space or to restore an intended, preplanned trajectory (Blouin et al. 2015). If these were the objectives of vestibular feedback in controlling arm movements, one would have expected the same corrective responses irrespective of the target condition. Instead, the observed reduction of corrective responses to the reduced accuracy requirements in the wide target condition seem to reflect a control policy that avoids unnecessary control effort (minimum intervention principle, Todorov and Jordan 2002). We argue that the earlier observed corrections in response to vestibular stimulation (see Blouin et al. 2015 for a review) were an emergent property of an optimal control policy with spatial target constraints along and perpendicular to the reach direction.

Our results fit with earlier observations of task-specific vestibular processing for postural control. In the legs, GVS-evoked responses are weaker if external support is provided (Britton et al. 1993; Fitzpatrick et al. 1994) or if stance width is increased (Day et al. 1997). Subjects can even adapt their response to GVS to an inverted relationship between balancing motor commands and associated vestibular feedback (Forbes et al. 2016). These results suggest that vestibular responses follow the minimum intervention principle in the case of balance control. In the upper limb, Smith and Reynolds (2017) have shown that responses to GVS are suppressed if the instruction is to keep pointing to a body-fixed target. Our results extend these findings, showing that this principle also applies to processing vestibular information during reaching movements. In our case, maintaining posture was not the prime behavioral goal especially because subjects were seated.

Although feedback corrections were larger for reaches to the narrow than the wide target, GVS clearly also evoked feedback corrections for the wide target, even though they were unnecessary to attain the goal. Similar residual responses have been observed for visual and mechanical perturbations (Knill et al. 2011; Nashed et al. 2012). It is possible that the more sophis-

ticated task-dependent modulation of feedback gains rides on top of a rudimentary task-independent response, like for mechanical arm perturbations (Pruszynski et al. 2011). The observed reduction of corrections by  $\sim 33\%$  in the wide condition is similar to the 40% reduction found for with visual cursor jumps when reaching to wide targets (Knill et al. 2011). This correspondence may hint at an alternative explanation for the residual response to the wide target. Nashed et al. (2012) pointed out that a controller that trades off between accuracy and effort should also show corrections in response to a perturbation along a task-irrelevant dimension to finally stabilize the hand at the target, which requires zero lateral velocity. Delaying this response would require more intense control commands, so it is optimal to respond immediately, though with appropriately reduced gain, even when reaching to the wide target. One way to test this experimentally is by asking subjects to reach through the target without stopping at it. In such “shooting movements,” the feedback responses should be further reduced.

Our finding of task-dependent vestibular feedback control and our interpretation in terms of optimized feedback gains is compatible with the view of predictive vestibular arm control (Blouin et al. 2015). OFC includes internal models for feed-forward prediction of future sensory input and for output generation based on inverse dynamics. Since vestibular signals inform the brain about head acceleration, their appropriate contributions to arm control requires integration with (neck) proprioception and a transformation into a trunk-fixed frame of reference (Cullen 2012; Mergner et al. 1997). Based on the estimated self-motion, an internal inverse model of the arm's biomechanics and resulting interaction torques allows the brain to generate appropriate control commands for the arm. These internal models have been shown to be very precise and flexible enough to account for varying hand loads and turning speeds in experiments with self-induced trunk rotations (Pigeon et al. 2003, 2013). Results of studies exposing subjects to rotation aftereffects (Bockisch and Haslwanter 2007) and from a deafferented subject (Blouin et al. 2010) suggest that this kind of predictive control can be elicited purely by vestibular input. In this vein, Moreau-Debord et al. (2014) used a computational model of arm biomechanics to account for the observed magnitude of arm responses to GVS, under the assumption that a current of 3 mA simulates a rotation speed of  $\sim 10^\circ/\text{s}$  (Fitzpatrick and Day 2004; Schneider et al. 2002). Their result suggests that the observed GVS-evoked responses are appropriate corrections for an illusory rotation, given that the brain uses an accurate inverse model of the arm's dynamics. With this level of sophistication in mind, it is straightforward to suggest that the brain combines postural control and reaching into a single feedback control policy. In line with this idea, Leonard et al. (2011) found that online arm corrections to visual target jumps in standing subjects are preceded by fast postural adjustments. In our study, an inferred postural perturbation was integrated into the accuracy requirements of an ongoing reach task. Together, these findings imply that the brain recruits feedback control policies based on all sensorimotor aspects of a task and can seamlessly coordinate between effectors.

Finally, we consider the physiological implications of our interpretation that vestibular inputs are processed by an optimal feedback reach controller. Within the framework of OFC,

online corrections result from a control policy that uses state estimates, built up by sensory feedback and internal predictions, to issue new motor commands. The only perturbed sensory inputs in our experiment were of vestibular origin and the corrections suggest that these vestibular signals are available to the state estimator. For reach control, state estimation involves the posterior parietal cortex (PPC, Shadmehr and Krakauer 2008), which is known to update its representations in response to visual (reviewed in Archambault et al. 2015) and proprioceptive (e.g., Omrani et al. 2016; Reichenbach et al. 2014) perturbations. Various studies have shown that the parietal cortex also receives vestibular information (Gutting et al. 2015; Shinder and Taube 2010; Ventre-Dominey 2014), but comparatively little is known about vestibular contributions to online reach control (Medendorp and Selen 2017). It has been argued that vestibular processing for online reach execution is distinct from vestibular-based updating of the internally represented target location (Bresciani et al. 2002c, 2005; Moreau-Debord et al. 2014). A recent study by Reichenbach et al. (2016) showed that transcranial magnetic stimulation of the ipsilateral (but not contralateral) PPC disrupts vestibular-evoked reach corrections to a passive full-body rotation, consistent with a state estimation process. However, a task-dependent response to these perturbations not only depends on dynamic state estimation but also requires tuning of the control policy, which has been tentatively associated with the (pre-)motor cortex (Shadmehr and Krakauer 2008). Indeed, the earliest task-dependent responses, a reflection the control policy, have been observed in primary motor cortex (Omrani et al. 2016). While our results suggest that vestibular signals influence the control policy of the ongoing reach, possibly through interaction with the state estimator of the limb, it is clear that more studies are needed to understand the physiological ramifications of our results.

In conclusion, we show that vestibular feedback corrections in goal-directed reaching are tuned to minimally intervene with the task-irrelevant dimension of the reach, implying an intimate integration of self-motion signals into online reach control.

## GRANTS

The research leading to these results has received funding from the European Union Seventh Framework Programme (FP7/2007–2013) under grant agreement no. 604063 (J. Keyser, W. P. Medendorp). The work has also been supported by the European Research Council, no. EU-ERC-283567 (W. P. Medendorp) and the Netherlands Organization for Scientific Research, no. NWO-VICI 453-11-001 (W. P. Medendorp) and no. NWO-VENI 451-10-017 (L. P. J. Selen).

## DISCLOSURES

No conflicts of interest, financial or otherwise, are declared by the authors.

## ENDNOTE

At the request of the author(s), readers are herein alerted to the fact that additional materials related to this manuscript may be found at the institutional website of one of the authors, which at the time of publication they indicate is: [http://hdl.handle.net/11633/di.dcc.DSC\\_2016.00215\\_976](http://hdl.handle.net/11633/di.dcc.DSC_2016.00215_976). These materials are not a part of this manuscript, and have not undergone peer review by the American Physiological Society (APS). APS and the journal editors take no responsibility for these materials, for the website address, or for any links to or from it.

## AUTHOR CONTRIBUTIONS

J.K., W.P.M., and L.P.S. conceived and designed research; J.K. performed experiments; J.K., W.P.M., and L.P.S. analyzed data; J.K., W.P.M., and L.P.S. interpreted results of experiments; J.K. prepared figures; J.K., W.P.M., and L.P.S. drafted manuscript; J.K., W.P.M., and L.P.S. edited and revised manuscript; J.K., W.P.M., and L.P.S. approved final version of manuscript.

## REFERENCES

- Archambault PS, Ferrari-Toniolo S, Caminiti R, Battaglia-Mayer A. Visually-guided correction of hand reaching movements: the neurophysiological bases in the cerebral cortex. *Vision Res* 110: 244–256, 2015. doi:10.1016/j.visres.2014.09.009.
- Blouin J, Bresciani J-P, Guillaud E, Simoneau M. Prediction in the vestibular control of arm movements. *Multisens Res* 28: 487–505, 2015. doi:10.1163/22134808-00002501.
- Blouin J, Guillaud E, Bresciani J-P, Guerraz M, Simoneau M. Insights into the control of arm movement during body motion as revealed by EMG analyses. *Brain Res* 1309: 40–52, 2010. doi:10.1016/j.brainres.2009.10.063.
- Bockisch CJ, Haslwanter T. Vestibular contribution to the planning of reach trajectories. *Exp Brain Res* 182: 387–397, 2007. doi:10.1007/s00221-007-0997-x.
- Bresciani J-P, Blouin J, Popov K, Bourdin C, Sarlegna F, Vercher J-L, Gauthier GM. Galvanic vestibular stimulation in humans produces online arm movement deviations when reaching towards memorized visual targets. *Neurosci Lett* 318: 34–38, 2002a. doi:10.1016/S0304-3940(01)02462-4.
- Bresciani J-P, Blouin J, Popov K, Sarlegna F, Bourdin C, Vercher J-L, Gauthier GM. Vestibular signals contribute to the online control of goal-directed arm movements [Online]. *Curr Psychol Cogn* 21: 263–280, 2002b. <https://hal.archives-ouvertes.fr/hal-00947249>.
- Bresciani J-P, Blouin J, Sarlegna F, Bourdin C, Vercher J-L, Gauthier GM. On-line versus off-line vestibular-evoked control of goal-directed arm movements. *Neuroreport* 13: 1563–1566, 2002c. doi:10.1097/00001756-200208270-00015.
- Bresciani J-P, Gauthier GM, Vercher J-L, Blouin J. On the nature of the vestibular control of arm-reaching movements during whole-body rotations. *Exp Brain Res* 164: 431–441, 2005. doi:10.1007/s00221-005-2263-4.
- Britton TC, Day BL, Brown P, Rothwell JC, Thompson PD, Marsden CD. Postural electromyographic responses in the arm and leg following galvanic vestibular stimulation in man. *Exp Brain Res* 94: 143–151, 1993. doi:10.1007/BF00230477.
- Crevecoeur F, Kurtzer I, Bourke T, Scott SH. Feedback responses rapidly scale with the urgency to correct for external perturbations. *J Neurophysiol* 110: 1323–1332, 2013. doi:10.1152/jn.00216.2013.
- Cullen KE. The vestibular system: multimodal integration and encoding of self-motion for motor control. *Trends Neurosci* 35: 185–196, 2012. doi:10.1016/j.tins.2011.12.001.
- Day BL, Séverac Cauquil A, Bartolomei L, Pastor MA, Lyon IN. Human body-segment tilts induced by galvanic stimulation: a vestibularly driven balance protection mechanism. *J Physiol* 500: 661–672, 1997. doi:10.1113/jphysiol.1997.sp022051.
- Fitzpatrick RC, Burke D, Gandevia SC. Task-dependent reflex responses and movement illusions evoked by galvanic vestibular stimulation in standing humans. *J Physiol* 478: 363–372, 1994. doi:10.1113/jphysiol.1994.sp020257.
- Fitzpatrick RC, Day BL. Probing the human vestibular system with galvanic stimulation. *J Appl Physiol* 96: 2301–2316, 2004. doi:10.1152/jappphysiol.00008.2004.
- Forbes PA, Luu BL, Van der Loos HF, Croft EA, Inglis JT, Blouin J-S. Transformation of vestibular signals for the control of standing in humans. *J Neurosci* 36: 11510–11520, 2016. doi:10.1523/JNEUROSCI.1902-16.2016.
- Franklin DW, Wolpert DM. Specificity of reflex adaptation for task-relevant variability. *J Neurosci* 28: 14165–14175, 2008. doi:10.1523/JNEUROSCI.4406-08.2008.
- Guillaud E, Simoneau M, Blouin J. Prediction of the body rotation-induced torques on the arm during reaching movements: evidence from a proprioceptively deafferented subject. *Neuropsychologia* 49: 2055–2059, 2011. doi:10.1016/j.neuropsychologia.2011.03.035.
- Gutting TP, Selen LPJ, Medendorp WP. Parallax-sensitive remapping of visual space in occipito-parietal alpha-band activity during whole-body motion. *J Neurophysiol* 113: 1574–1584, 2015. doi:10.1152/jn.00477.2014.
- HDF Group. *Hierarchical Data Format, version 5*. 1997–2017. <https://www.hdfgroup.org/>.



- Howard IS, Ingram JN, Wolpert DM. A modular planar robotic manipulator with end-point torque control. *J Neurosci Methods* 181: 199–211, 2009. doi:10.1016/j.jneumeth.2009.05.005.
- Hunter JD. Matplotlib: a 2D graphics environment. *Comput Sci Eng* 9: 90–95, 2007. doi:10.1109/MCSE.2007.55.
- Jones E, Oliphant T, Peterson P, others. SciPy: Open source scientific tools for Python [Online]. 2001–2017. <https://www.scipy.org/>.
- Knill DC, Bondada A, Chhabra M. Flexible, task-dependent use of sensory feedback to control hand movements. *J Neurosci* 31: 1219–1237, 2011. doi:10.1523/JNEUROSCI.3522-09.2011.
- Leonard JA, Gritsenko V, Ouckama R, Stapley PJ. Postural adjustments for online corrections of arm movements in standing humans. *J Neurophysiol* 105: 2375–2388, 2011. doi:10.1152/jn.00944.2010.
- Mars F, Archambault PS, Feldman AG. Vestibular contribution to combined arm and trunk motion. *Exp Brain Res* 150: 515–519, 2003. doi:10.1007/s00221-003-1485-6.
- Medendorp WP, Selen LJP. Vestibular contributions to high-level sensorimotor functions. *Neuropsychologia* S0028-3932(17)30050-7, 2017. doi:10.1016/j.neuropsychologia.2017.02.004.
- Mergner T, Huber W, Becker W. Vestibular-neck interaction and transformation of sensory coordinates. *J Vestib Res* 7: 347–367, 1997. doi:10.1016/S0957-4271(96)00176-0.
- Moreau-Debord I, Martin CZ, Landry M, Green AM. Evidence for a reference frame transformation of vestibular signal contributions to voluntary reaching. *J Neurophysiol* 111: 1903–1919, 2014. doi:10.1152/jn.00419.2013.
- Nashed JY, Crevecoeur F, Scott SH. Influence of the behavioral goal and environmental obstacles on rapid feedback responses. *J Neurophysiol* 108: 999–1009, 2012. doi:10.1152/jn.01089.2011.
- Omrani M, Murnaghan CD, Pruszynski JA, Scott SH. Distributed task-specific processing of somatosensory feedback for voluntary motor control. *eLife* 5: e13141, 2016. doi:10.7554/eLife.13141.
- Oostwoud Wijdenes L, Brenner E, Smeets JBJ. Fast and fine-tuned corrections when the target of a hand movement is displaced. *Exp Brain Res* 214: 453–462, 2011. doi:10.1007/s00221-011-2843-4.
- Oostwoud Wijdenes L, Brenner E, Smeets JBJ. Analysis of methods to determine the latency of online movement adjustments. *Behav Res Methods* 46: 131–139, 2014. doi:10.3758/s13428-013-0349-7.
- Pigeon P, Bortolami SB, DiZio P, Lackner JR. Coordinated turn-and-reach movements. I. Anticipatory compensation for self-generated coriolis and interaction torques. *J Neurophysiol* 89: 276–289, 2003. doi:10.1152/jn.00159.2001.
- Pigeon P, Dizio P, Lackner JR. Immediate compensation for variations in self-generated Coriolis torques related to body dynamics and carried objects. *J Neurophysiol* 110: 1370–1384, 2013. doi:10.1152/jn.00104.2012.
- Pruszynski JA, Kurtzer I, Scott SH. Rapid motor responses are appropriately tuned to the metrics of a visuospatial task. *J Neurophysiol* 100: 224–238, 2008. doi:10.1152/jn.90262.2008.
- Pruszynski JA, Kurtzer I, Scott SH. The long-latency reflex is composed of at least two functionally independent processes. *J Neurophysiol* 106: 449–459, 2011. doi:10.1152/jn.01052.2010.
- R Core Team. R: a language and environment for statistical computing [Online]. R Foundation for Statistical Computing. <https://www.R-project.org>, 2016.
- Reichenbach A, Bresciani J-P, Bühlhoff HH, Thielscher A. Reaching with the sixth sense: Vestibular contributions to voluntary motor control in the human right parietal cortex. *Neuroimage* 124: 869–875, 2016. doi:10.1016/j.neuroimage.2015.09.043.
- Reichenbach A, Thielscher A, Peer A, Bühlhoff HH, Bresciani J-P. A key region in the human parietal cortex for processing proprioceptive hand feedback during reaching movements. *Neuroimage* 84: 615–625, 2014. doi:10.1016/j.neuroimage.2013.09.024.
- Reynolds RF, Osler CJ. Galvanic vestibular stimulation produces sensations of rotation consistent with activation of semicircular canal afferents. *Front Neurol* 3: 104, 2012. doi:10.3389/fneur.2012.00104.
- Schneider E, Glasauer S, Dieterich M. Comparison of human ocular torsion patterns during natural and galvanic vestibular stimulation. *J Neurophysiol* 87: 2064–2073, 2002. doi:10.1152/jn.00558.2001.
- Scott SH. Optimal feedback control and the neural basis of volitional motor control. *Nat Rev Neurosci* 5: 532–546, 2004. doi:10.1038/nrn1427.
- Shadmehr R, Krakauer JW. A computational neuroanatomy for motor control. *Exp Brain Res* 185: 359–381, 2008. doi:10.1007/s00221-008-1280-5.
- Shinder ME, Taube JS. Differentiating ascending vestibular pathways to the cortex involved in spatial cognition. *J Vestib Res* 20: 3–23, 2010. doi:10.3233/VES-2010-0344.
- Smith CP, Reynolds RF. Vestibular feedback maintains reaching accuracy during body movement. *J Physiol* 595: 1339–1349, 2017. doi:10.1113/JP273125.
- Todorov E, Jordan MI. Optimal feedback control as a theory of motor coordination. *Nat Neurosci* 5: 1226–1235, 2002. doi:10.1038/nrn963.
- van der Walt S, Colbert SC, Varoquaux G. The NumPy array: a structure for efficient numerical computation. *Comput Sci Eng* 13: 22–30, 2011. doi:10.1109/MCSE.2011.37.
- Veerman MM, Brenner E, Smeets JBJ. The latency for correcting a movement depends on the visual attribute that defines the target. *Exp Brain Res* 187: 219–228, 2008. doi:10.1007/s00221-008-1296-x.
- Ventre-Dominey J. Vestibular function in the temporal and parietal cortex: distinct velocity and inertial processing pathways. *Front Integr Neurosci* 8: 53, 2014. doi:10.3389/fnint.2014.00053.